

Article

Optimizing Solar Parabolic Trough Receivers with External Fins: An Experimental Study on Enhancing Heat Transfer and Thermal Efficiency [†]

Teerapath Limboonruang ^{1,*} , Muyiwa Oyinlola ¹ , Dani Harmanto ¹, Pracha Bunyawichakul ² and Nittalin Phunapai ²

¹ Institute of Energy and Sustainable Development (IESD), De Montfort University, Leicester LE1 9BH, UK; muyiwa.oyinlola@dmu.ac.uk (M.O.); dani.harmanto@dmu.ac.uk (D.H.)

² Innovative Development, Automation System and Sustainability Laboratory (I-DASS Lab), Department of Mechanical Engineering, Faculty of Engineering, Srinakharinwirot University, Bangkok 10110, Thailand; prachabu@swu.ac.th (P.B.); nittalin@swu.ac.th (N.P.)

* Correspondence: p2558151@my365.dmu.ac.uk; Tel.: +44-782-449-2049

[†] This paper is an extended version of our paper published in 2022, International Conference on Heat Transfer, Fluid Mechanics and Thermodynamics (HEFAT-ATE 2022), Amsterdam, The Netherlands, 8–10 August 2022; pp. 432–437.

Abstract: Several researchers have shown that the heat transfer performance of solar parabolic trough (SPT) receivers may be improved by increasing their surface area or by adding internal fins to the tubes. Unfortunately, the manufacture of internally finned tubes involves complex processes, resulting in significant cost increases. On the other hand, the addition of external fins to tubes is more technically and economically feasible in a low-resource setting. This study investigates the potential benefits of integrating external fins on the receiver tubes of a low-cost SPT collector system. Experiments were conducted using an SPT system with a focal length of 300 mm and a collector length of 5.1 m, and they were positioned by an automated Sun tracking system. Tests were undertaken using both smooth and externally finned receiver tubes operating at five different water flow rates. The solar receiver with a finned tube was able to provide a maximum water temperature of 59.34 °C compared with that of 56.52 °C for a smooth tube at a flow rate of 0.5 L per minute. The externally finned absorber tube was also found to have a maximum efficiency of 18.20% at an average daily solar intensity of 834.61 W/m², which is approximately 48% more efficient than the smooth tube. The calculations indicate that the experimental SPT system using finned tubes potentially avoids 0.2726 metric tons of CO₂e per year, with finned tubes outperforming smooth tubes by up to 44%. The results show that using externally finned receiver tubes can significantly enhance the thermal performance of SPT collector systems.

Keywords: solar parabolic trough; solar energy; absorber tubes; renewable energy; fins tube



Citation: Limboonruang, T.; Oyinlola, M.; Harmanto, D.; Bunyawichakul, P.; Phunapai, N. Optimizing Solar Parabolic Trough Receivers with External Fins: An Experimental Study on Enhancing Heat Transfer and Thermal Efficiency. *Energies* **2023**, *16*, 6520. <https://doi.org/10.3390/en16186520>

Academic Editors: Gianpiero Colangelo, Meng Lin, Ligang Wang and Ruikai Zhao

Received: 23 June 2023

Revised: 27 August 2023

Accepted: 7 September 2023

Published: 10 September 2023



Copyright: © 2023 by the authors. Licensee MDPI, Basel, Switzerland. This article is an open access article distributed under the terms and conditions of the Creative Commons Attribution (CC BY) license (<https://creativecommons.org/licenses/by/4.0/>).

1. Introduction

The energy sector in Thailand depends heavily on imported oil and gas products. The current situation of dramatic increases in global crude oil prices and the increased demand for energy have put the country in a tough economic situation and reduced economic growth. Therefore, it is important to find alternative energy sources that guarantee the security of the supply. Solar energy has the greatest potential of all the sources of renewable energy [1–6]; therefore, with the limited supply of fossil fuels, the increased use of solar energy has become inevitable. Thailand is located near the equator and has a high potential for harnessing solar energy compared with other countries [7]. In fact, Thailand lies in a region of high solar insolation, where the average insolation intensity on a horizontal surface is approximately 1367 W/m² [3,8], giving an enormous daily energy of 5–7 kWh/m²/d,

which is one of the highest in the world [3,9,10]. This presents an opportunity for energy independence and a better future for Thailand.

Solar thermal power plants using concentration technologies are important candidates for providing the bulk solar electricity needed within the next few decades [11,12]. Solar collectors for high temperatures require concentration systems, such as parabolic reflectors. Solar parabolic trough (SPT) systems have been proven to work, and they consist of large fields of parabolic trough collectors with a heat transfer fluid/steam generation system. A parabolic trough solar collector uses a mirror in the shape of a parabolic cylinder to reflect and concentrate the radiation from the Sun toward a solar receiver tube located at the focus line of the parabolic cylinder [10,13–15]. The solar receiver tube absorbs the incoming radiation and transforms it into thermal energy, which is collected and transported by a fluid medium circulating within the receiver tube. This method of concentrated solar collection has the advantage of high efficiency and can be used either for thermal energy collection, for generating electricity [16], or for both; therefore, it is an important way to exploit solar energy directly [17]. Furthermore, several studies have shown that solar concentrating plants have great prospects in terms of a low environmental impact and favorable techno-economic factors [18–21]. For example, thanks to the use of solar concentrator power plants, India has avoided around 170,000 metric tons of CO₂e per year [19], and Pakistan has avoided over 225,000 metric tons of CO₂e per year [21]. Unfortunately capital costs for parabolic collectors are quite high; for example, a 250 MW parabolic solar power plant in the United States costs USD 1.6 billion to build [22]. In Thailand [23], a budget of THB 900 million (approximately USD 30 million) is required for the construction of a 5 MW parabolic solar power plant. Therefore, it is important to explore opportunities to reduce costs, such as the development of the local capacity and the capability to innovate using local materials.

Several studies have been undertaken in an effort to improve PTCs' performance, such as through modifications to the geometry [24–29], enhancing the working fluids [30–32], introducing absorber tube coatings [33–35], and adding tracker systems [36–38]. The study reported in this paper focuses on improving the thermal performance by modifying the geometry, specifically, by using the principle that the heat absorption of the solar receivers increases with an increase in the heat transfer area [28,31]. A common method of modifying the geometry is increasing the heat transfer area between the solar receiver tube and heat transfer fluid [39,40], which results in better overall heat absorption. As a result, thermal performance enhancement is accomplished by manipulating properties such as the system's geometry; by adding artificial roughness [24–26], fins [27–29], baffles [41–43], wires [44–46], swirling devices [47–49], and vortex generators; or by manipulating the material of the absorber tube [50–52] and the fluid properties [32,53,54].

Several studies have shown that internal fins can enhance heat transfer. Huang, Yu [26] used a computational simulation to study the effect of increasing the surface area inside the absorber tube by using tubes with dimples or protrusions. Bellos, Tzivanidis [30] developed a finned absorber inside the tube to enhance the thermal efficiency. Peng, Li [27] and Zhao, Bai [29] studied the impact of various fin shapes on the heat transfer and performance of solar absorber tubes. Improving a solar receiver tube by changing the geometry and adding fins enhances the thermal efficiency. However, the processes required to manufacture internally finned tubes are difficult and complicated, leading to high production costs, which are incompatible with a low-income setting. Therefore, building on the principle that external fins will increase the surface area for absorbing solar radiation, this study experimentally examines the potential of using external fins to improve the thermal performance of an SPT. While the literature has many examples of internal fins, examples of external fins are limited. A few studies have used external fins, such as Gong, Wang [14], who used computational simulations to study the fins' shape in an absorber tube (AT) and found that the thermal efficiency of the tube appeared to improve from 75.7% to 76.9% with short, thick AT fins, which increased heat transmission in the AT compared to the finless AT. However, thin and long fins create more frictional

loss than wide and short fins due to the length of the tube. A computational study by Gong, Wang [13] led to an improved AT design using hemispherical external fins with flat radiation shielding inside the evacuation ring of the PTC system. It was found that the optical and thermal efficiency was 8% higher than that with the traditional AT design. Even though these computational studies show satisfactory performance results for externally finned absorber tubes, experimental studies are scarce in the literature. Furthermore, none of the previous studies included an economic and environmental assessment of a simple low-cost manufacturing process. This study aims to fill this gap in the design and development of a solar parabolic trough collector system suitable for manufacture in Thailand. It achieves this by experimentally investigating the effects of external fins on the performance of absorber tubes. It provides insight into the temperature of the outflow water, heat transfer, and efficiency as well as an evaluation of the economic and environmental aspects of the system.

2. Materials and Methods

2.1. Basic Concepts of the Parabola and Earth–Sun Angles

The parabolic trough solar collector was constructed by using mirrors in the shape of a parabolic cylinder to reflect and concentrate solar radiation onto an absorber tube located at the focal line of the parabolic cylinder. The absorber tube absorbed the incoming solar radiation and transformed it into thermal energy. A conceptual schematic of the design of the component of the parabolic shape [55] is shown in Figure 1.

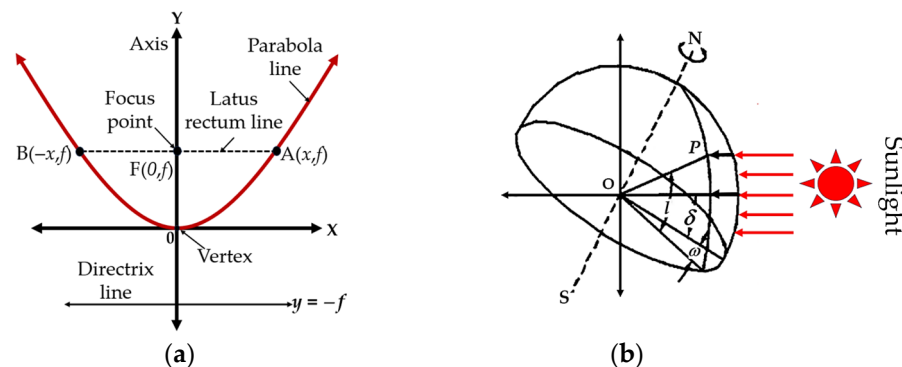


Figure 1. Basic concepts of (a) the parabola and (b) the Earth–Sun angles.

The equation for the parabolic trough in cylindrical coordinates is [56]

$$y = \frac{x^2}{4f} \quad (1)$$

The reflector of a suitable parabolic design typically has focal length (f) to aperture width (W) ratio of about 0.25 as calculated from the equation [56]

$$\frac{f}{W} = 0.25 \quad (2)$$

The geometric concentration ratio (CR) of the parabolic trough collector is calculated from the equation [57]

$$CR = \frac{\text{Aperture area}}{\text{Receiver area}} = \frac{W - D_r}{\pi D_r} \quad (3)$$

The surface area of the solar receiver (A_r) tube is calculated from the equation

$$A_r = \pi D_r L_r \quad (4)$$

where D_r is receiver diameter and where L_r is receiver length.

On the basis of determining the position of point P on the Earth's surface in relation to the solar radiation, the parameters required for the design of a solar tracking system can be calculated at any instant if the latitude (l), the hour angle (w), and the Sun's declination angle (d) are known for that point [8,10,55] as shown in Figure 1. Declination angle (d) is the angular position of the Sun at solar noon compared with the equator, which is $23.45^\circ \leq \delta \leq 23.45^\circ$ as computed using

$$\delta = 23.45 \sin \left(360 \times \frac{284 + n}{365} \right) \quad (5)$$

The angle of each hour (w) is obtained from

$$\omega = 15(12 - st) \quad (6)$$

The local standard time (st) compared with solar noon, an area test, is obtained from

$$st = \text{Standard time} + E - 4(\text{Long}_{st} - \text{Long}_{Loc}) \quad (7)$$

2.2. Experimental Setup

The experimental system described in Limboonruang et al. [55] was used to conduct the experiments. The solar parabolic trough collector (SPTC) system was set up with the long axis of the parabola oriented along the north–south direction. The parabolic trough would therefore collect solar radiation in the east–west direction. The experimental system comprised three SPTs as shown in Figure 2, each measuring $1200 \times 1520 \text{ mm}^2$ with a 300 mm focal length, which concentrated sunlight at the focal point. The components of the collector and solar parabolic trough assembly were as follows: (i) solar receiver vacuum tube, (ii) solar parabolic trough collector, (iii) solar hot water tank, and (iv) Sun tracking system. The components and schematic diagram of the system are shown in Figure 2. The solar tracking system for the SPT is shown in Figure 3, and the characteristics of the SPT are shown in Table 1.

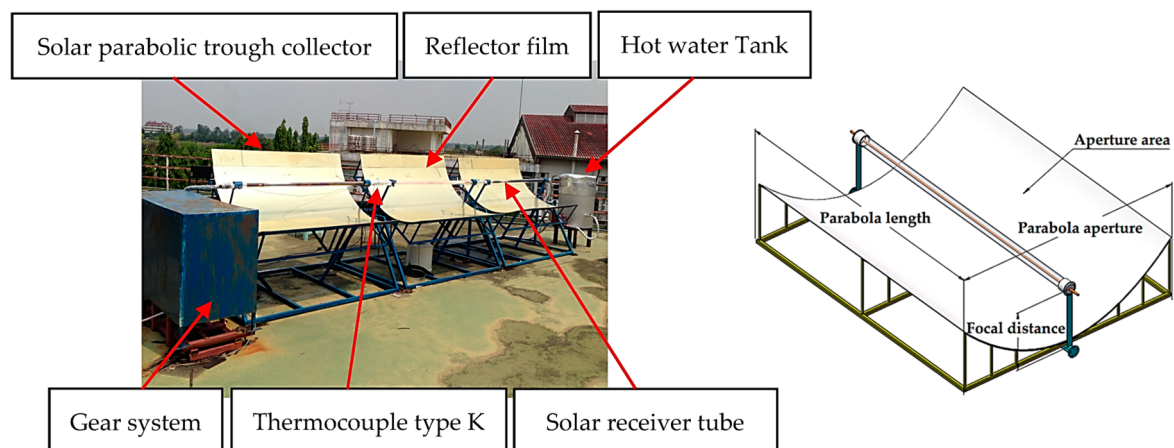


Figure 2. The solar parabolic trough collector and schematic diagram of the SPTC [55].

The components and geometric parameters of the solar absorber vacuum tube assembly used for the experiment are shown in Figure 4. Two types of absorber tubes were evaluated, specifically, (a) smooth copper tubes and (b) finned copper tubes. The absorber tubes were mounted coaxially within an evacuated glass tube. The vacuum enclosure reduced thermal losses from the absorber tube. The design parameters of the tubes are shown in Table 2.

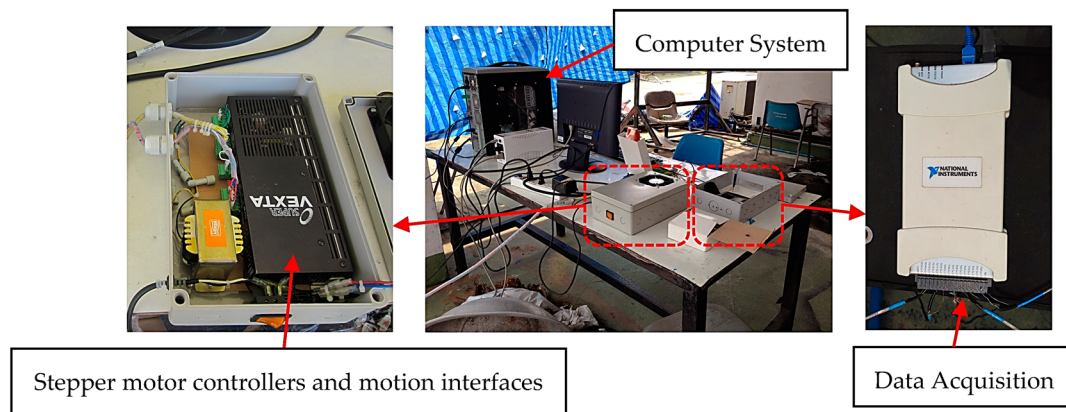


Figure 3. The solar tracking and data acquisition systems for the SPTC [55].

Table 1. Characteristics of each solar parabolic trough collector (SPTC) set.

No.	Parameter	Characteristics
1	Parabola length (L)	1520 mm
2	Parabola aperture (W)	1200 mm
3	Focal distance (f)	300 mm
4	Thickness (mean value)	3 mm
5	Aperture area (A_a)	2.09 m ²
6	Collector length (L)	1.52 m
7	Concentration ratio (CR)	8.13

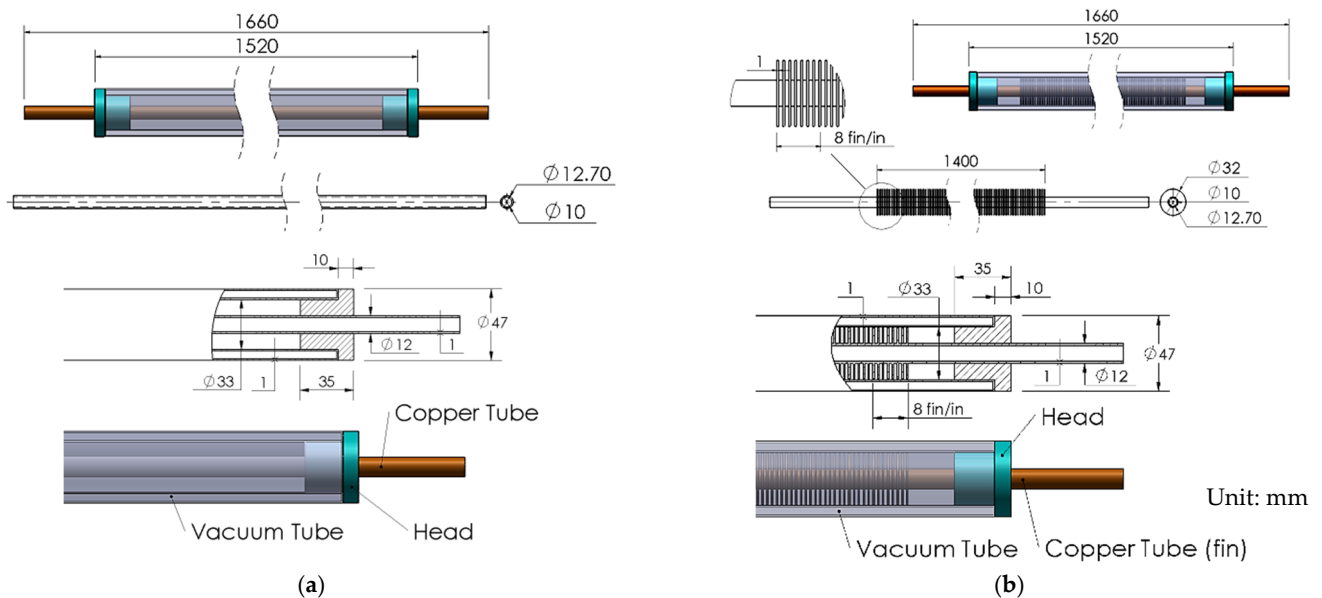
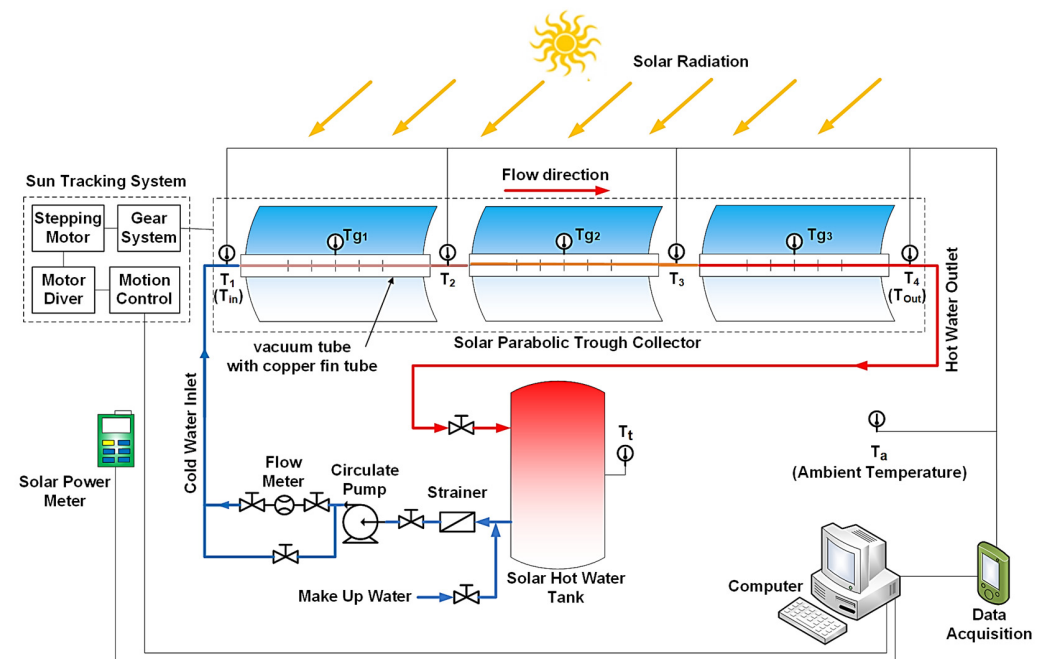
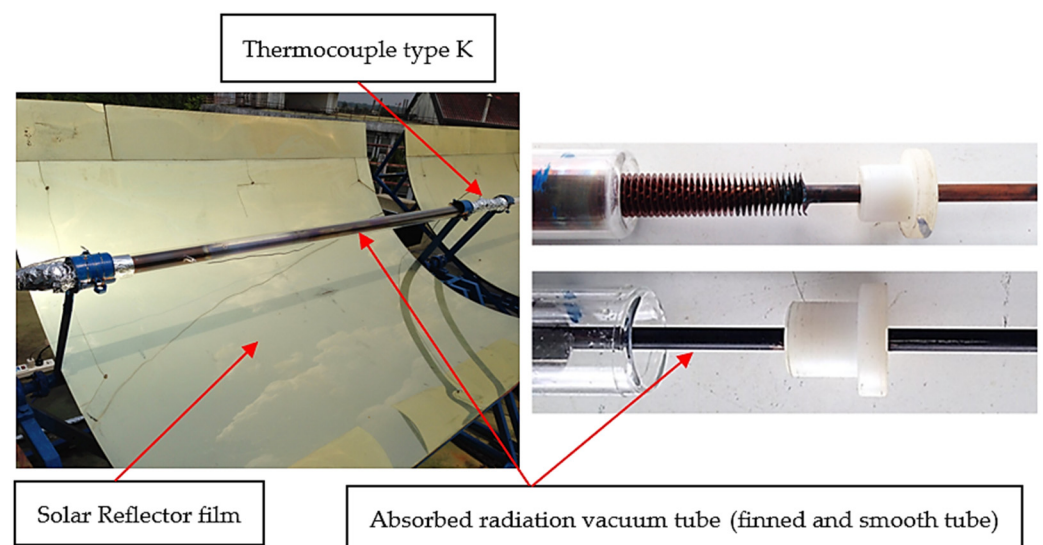


Figure 4. Geometrical parameters of the solar receiver tubes: (a) smooth copper tube and (b) finned copper tube.

The temperature of the circulating heat transfer fluid (in this case, water) was measured at the test points, T_1 to T_4 , on the absorber tubes, and the local ambient air temperature (T_a) was also measured. The distance between the measurement points, T_1 , T_2 , T_3 , and T_4 , was 1.7 m as shown in Figure 5. The absorber tube's glass envelope had an external diameter of 47 mm and an internal diameter of 33 mm. The copper absorber tube was mounted coaxially within the glass envelope, and the envelope was evacuated to help retain heat as shown in Figure 6.

Table 2. Parameters of the solar receiver tubes.

No.	Parameter	Volume/Type
1	Receiver material	copper
2	Receiver surface treatment	Heat-resistant black coating
3	Inner copper tube diameter (D_{ci})	10 mm
4	Outer copper tube diameter (D_{co})	12.70 mm
5	Inner glass cover diameter (D_{gi})	33.50 mm
6	Outer glass cover diameter (D_{go})	47 mm
7	Glass envelope transmissivity	0.95
8	Receiver length (L_r)	1.52 m
9	Receiver surface area (A_r)	0.23 m ²

**Figure 5.** Schematic diagrams of experimental apparatus.**Figure 6.** Absorber vacuum tube assemblies for smooth and finned tubes.

The heat transfer fluid (HTF) used in this experiment was water supplied from a 60-L storage tank. Water's physical properties are listed in Table 3. The controlled variable in the

experiment was the flow rate of the water, specifically, flow rates of 0.5, 1, 2, 3, and 4 L per minute. Data collection was undertaken between the hours of 10:00 and 16:00 local time. The temperature at each test point (T_1 to T_4) and the air temperature (T_a) were measured using type K thermocouples connected to a National Instruments NI-9213 (Manufactured by Apex Waves, NC, USA) data acquisition system and were recorded every minute. A TES-1333R solar power meter (Manufactured by TES Electrical Electronic Corp, Taipei, Taiwan), which has an accuracy of $\pm 5\%$ according to the manufacturer, was set up beside the SPT and was used to measure the local direct solar light intensity (I_b) in units of W/m^2 once every minute. The flow rate was measured using a Well PRZ-15 (Manufactured by Pako Engineering Company Limited, Bangkok, Thailand) flow meter, which was connected to the piping system after the circulating pump and controlled the mass flow rate of the working fluid by adjusting the ball valve. The experiment was conducted over ten days in Nakhon Nayok Province, Thailand.

Table 3. Thermal properties of water at 25 °C.

No.	Parameter	Volume
1	Density (ρ)	997 kg/m ³
2	Boiling point	100 °C
3	Specific heat capacity (C_p)	4180 J/(kg °C)
4	Dynamic viscosity (μ)	0.95×10^{-3} kg/m s
5	Thermal conductivity (k)	0.60 W/(m °C)

2.3. The Solar Tracking System

The SPT system is located in Nakhon Nayok Province, Thailand, at a longitude of 101.00° E and a latitude of 14.12° N. The time zone is UTC + 07, and its proximity to the equator makes it strategically placed. During experiments, the SPT system was positioned with its parabolic trough's long axis aligned along the north–south direction. This positioning allowed the trough to collect solar radiation in the east–west direction throughout the experiment. The solar tracking system, shown in Figure 3, controlled the movement of the SPT unit. The solar tracking control system was created using LabVIEW version 2010 and was based on Equations (5)–(7), enabling the programming of position and time settings. The SPT was initially oriented east as the starting position. To start the program, the user had to input the location, time zone, and local time into the software. Once these settings were in place, the program was ready to operate. The system then tracked the daily trajectory of the Sun by rotating the SPT axis from east to west at a constant speed of 0.00415 degrees per second using a stepping motor (ORIENTAL model PH599-A, Manufactured by ORIENTAL MOTOR CO., LTD., Tokyo, Japan) connected to a gearbox designed for a total rotation of 15 degrees per hour [56]. At the end of the day, the SPT returned to its starting position.

The experiment was conducted from 11 to 30 March during Thailand's summer season. This corresponded to day numbers (n) 70 to 89 for the year. Using Equation (5), the declination angle (δ) of the Sun was calculated to be between -4.41° and 3.22° . Equation (8) [56] illustrates the angle of incidence for the SPT on a north–south axis with a continuous east-to-west trajectory. The resulting calculation showed an angle of $0.997 \leq \cos\theta \leq 0.998$.

$$\cos\theta = \cos\delta \quad (8)$$

where θ is the Sun's incident angle and where δ is the Sun's declination angle.

The concentrating solar system involved a horizontal single-axis solar tracking control system. As a result, the incident angle of the Sun (θ) had an impact on the aperture area's effective daylight area (A_d). This is demonstrated in Figure 7. To calculate the effective intensity of sunlight falling on the collection area, it was important to take into account

the solar intensity on the aperture area and the variable angle of incidence due to seasonal changes. This can be done using Equation (9) [58].

$$I_{eff} = I_b \cos \theta \quad (9)$$

where I_{eff} is the effective intensity of sunlight falling on the collection area, I_b is the local direct solar light intensity, and θ is the Sun's incident angle. Based on the above equations, the effective intensity of solar radiation was $0.997I_b \leq I_{eff} \leq 0.998I_b$, indicating a close approximation to direct solar radiation. Therefore, one may use $I_{eff} \approx I_b$ to simplify calculations in this experiment.

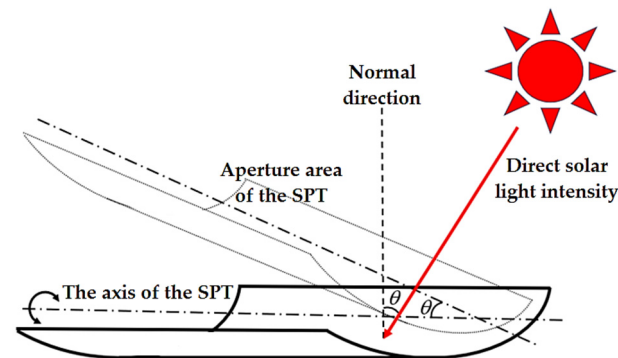


Figure 7. The effect of the angle of incidence of the Sun on the aperture area.

2.4. Data Reduction

Average hourly data from all instruments were computed and used for analysis. The equations and the parameters used when processing the data are summarized in Table 4.

Table 4. Details of parameters and equations used in data reduction.

Parameter	Relation	Units	Equation No.
Mean glass receiver tube temperature	$T_g = \frac{\sum_{i=1}^n T_{gi}}{n}$	°C	(10)
The mean fluid temperature [28]	$T_{fm} = \frac{T_1 + T_4}{2}$	°C	(11)
Solar energy on the trough aperture [59]	$Q_s = \alpha A_a I_b$	W	(12)
Heat absorbed	$Q = \dot{m} C_p (T_4 - T_1)$	W	(13)
Daily energy gained by water [60]	$Q_{water} = \dot{m} C_p (T_{final} - T_{initial})$	kJ	(14)
Overall efficiency	$\eta = \frac{\dot{m} C_p (T_{final} - T_{initial})}{\alpha A_a I_b}$	-	(15)
Water velocity	$v = \frac{\dot{V}}{A_c}$	m/s	(16)
Reynolds number	$Re = \frac{\rho v D_{ci}}{\mu}$	-	(17)

2.5. Economic Evaluation

A financial cost and revenue analysis of the SPT system was undertaken using the initial project cost and net present cost (C_{NPC}). This was used to determine the economic viability of the SPT system in order to estimate the project value by analyzing the investment value. This included the project's payback period (PB), net present value (NPV), and internal rate of return (IRR).

The net present cost (C_{NPC}) can be calculated using the equation [61]

$$C_{NPC} = \frac{C_{TALC}}{CRF(i, N)} \quad (18)$$

where C_{TALC} is the total annualized cost (*USD/year*) and where $CRF(i, N)$ is the capital recovery factor for the STP system for this case study, which can be calculated as [61]

$$CRF(i, N) = \frac{i(1+i)^N}{(1+i)^N - 1} \quad (19)$$

where N is the product's lifetime (*year*) and where i is the actual interest rate (%).

The net present value (*NPV*) can be estimated using the equation [62,63]

$$NPV = \sum_{i=1}^n \frac{R_i}{(1+r)^i} - \text{Initial investment} \quad (20)$$

where R_i is the cash flow for i period, n is the life of the SPT system project (*year*), and r is discount rate, and the internal rate of return (*IRR*) can be shown as follows in Equation (21) [62,63]:

$$\sum_{i=1}^n \frac{R_i}{(1+IRR)^i} - \text{Initial investment} = 0 \quad (21)$$

To estimate the payback period (*PB*), one must know the initial investment and the duration of the asset's expected cash flow. The following formula (22) [62,63] is used to calculate the *PB*:

$$PB = \frac{\text{Initial investment}}{\text{Expected annual cash inflow}} \quad (22)$$

2.6. Uncertainty Analysis

This section presents the experiment's inherent uncertainties. The solar power meter, type K thermocouples, flow meter, and data acquisition were used to collect the various types of data from the experiment. The standard uncertainty (F_z) of the parameters in the data calculation can be computed using Equation (23), where Y_z is the accuracy of the devices [64], and the uncertainty $X_{(b)}$ can be computed using Equation (24) [64]:

$$F_z = \frac{Y_z}{\sqrt{3}} \quad (23)$$

$$X_{(b)} = \sqrt{\frac{(\text{Uncertainty of Solar power meter})^2 + (\text{Uncertainty of Thermocouple})^2 + (\text{Uncertainty of Flow meter})^2 + (\text{Uncertainty of Data logger})^2}{4}} \quad (24)$$

Table 5 provides each device's accuracy and uncertainty. As a result, the overall uncertainty error for the experiment was 3.06%.

Table 5. Accuracy and uncertainty of measuring instruments.

Instrument	Units	Range	Accuracy (%)	Uncertainty (%)
Solar power meter	W/m ²	0–2000	±5	±2.886
Thermocouple type K	°C	−270 to 1260	±0.75	±0.433
Flow meter	Liters per minute	0.0 to 4.0	±1.6	±0.924
Data logger acquisition	°C	-	<0.02	±0.011

3. Results and Discussion

This experiment aims to compare the thermal performance of solar absorbers fitted with (a) smooth and (b) externally finned tubes. The primary variable studied in this experiment is the flow rate of the heat transfer fluid in the absorber tubes.

3.1. Solar Radiation with Time

Figure 8 shows the variation in solar radiation with time. The experiment was conducted over 20 days. The complete experimental data for solar radiation over 20 days on clear and cloudy days are shown in Figure A1. However, only the data from the 10 days with the least cloud cover were selected for processing as shown in Figure 8. It is pertinent to note that, on all days, the total amount of solar energy received by the collector was almost identical. As expected, solar radiation is time-dependent, with a sharp rise between 10:00 and 11:00. During the morning period, solar radiation ranged from 474.45 to 1127.84 W/m², reaching a maximum between 11:00 and 13:00 and then beginning to fall from 13:00 to 16:00. The average solar radiation observed was 834.61 W/m² over the 10 days selected for the experiment. This solar radiation profile is typical for around 8–10 months per year in Thailand [65,66], illustrating that the PTC will perform well through the majority of the year. However, in practical applications, the measured solar power values can vary over time due to other atmospheric factors, such as wind, pollution, and atmospheric dust. These factors can all result in a decrease in the fraction of solar radiation reaching the collector.

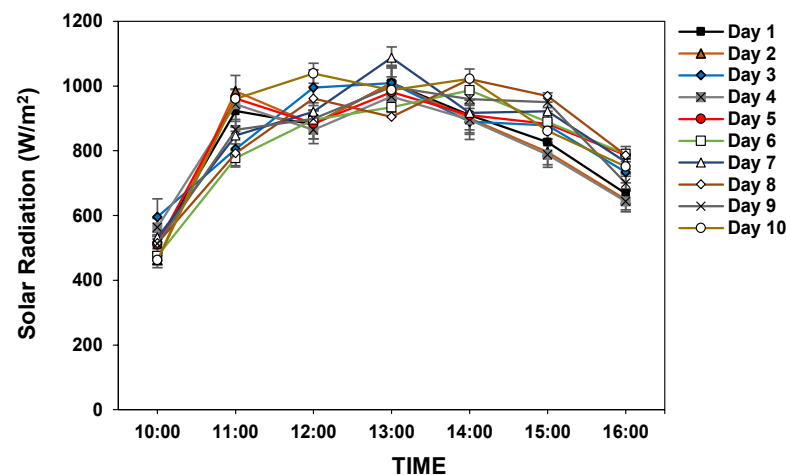


Figure 8. Variation in solar radiation with time.

3.2. Outlet Water Temperature

Figure 9 shows the effect of varying the flow rate of the water in the smooth and finned copper absorber tubes. The data were obtained by running the experiments at different flow rates, ranging from 0.5 to 4 L per minute. As expected, the fluid outlet temperature decreased with an increase in the flow rate, and it can be observed that the finned tubes consistently provided a higher outlet temperature than the smooth tubes at the same flow rate. It can be seen that a maximum outlet temperature of 56.52 °C at 0.5 L per minute was achieved for a smooth tube, and a maximum outlet temperature of 59.34 °C at 0.5 L per minute was achieved for a finned tube. The average daily ambient air temperature was 38.20 °C. Therefore, the results show the effect of the mass flow rate and temperature difference. Higher temperature differences result from lower mass flow rates because the working fluid spends a longer time receiving energy at a lower water velocity. Since the primary function of the SPT collector is to provide heat, running the collector at a lower flow rate is more beneficial in terms of higher outlet temperatures. Furthermore, because a lower flow rate implies a reduced pumping power requirement, the overall system efficiency improves as shown in a prior study [67,68]. However, a solar receiver at a higher temperature implies a higher rate of heat loss from the solar absorber. As indicated in previous studies [28,69], heat loss can be reduced by installing insulation on the solar receiver's surface, which will decrease the temperature of the solar receiver and minimize the overall heat loss.

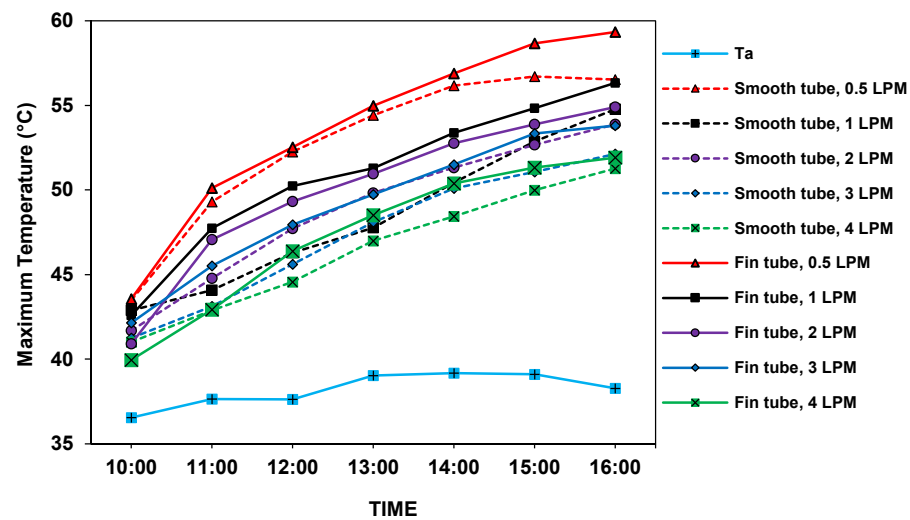


Figure 9. Comparison of outlet water temperature with time at various flow rates for smooth and finned tubes.

Figure 10 shows the smooth and finned copper absorber tubes' maximum output water temperature as a function of the water flow rate. Table 6 compares the outlet water temperatures of the smooth and finned tubes. It can be observed that the externally finned copper tubes delivered higher temperatures than the smooth copper tubes at all the flow rates studied. With a flow rate of 0.5 L per minute, the maximum output temperature of the finned tube was 59.34 °C; this is 2.82 °C more than that of the smooth copper tube, representing a 4.75% increase. When the flow rate was increased, the output temperature decreased for both types of tubes. It should be noted that some of the abnormal data shown in Figures 9 and 10 were due to the occasional passing of clouds and changes in wind, which caused fluctuations in the effective solar intensity and affected the outlet water temperature. However, the graphs' trends returned to normal after the clouds passed.

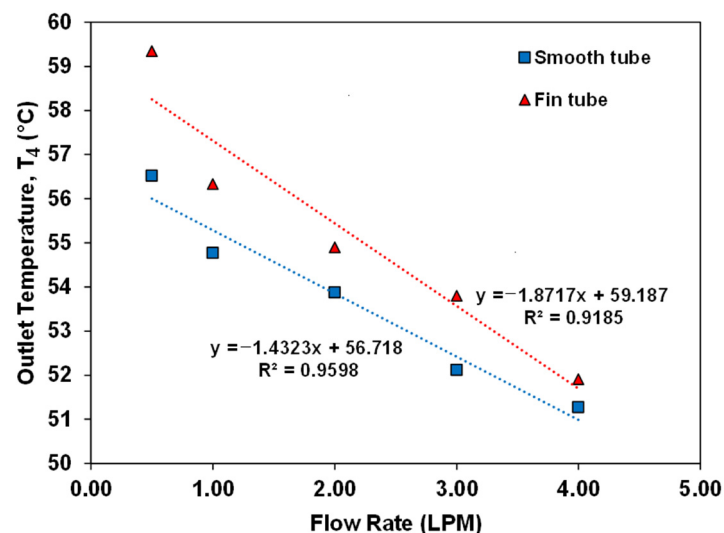


Figure 10. Variation in maximum outlet water temperature with flow rate.

Figure 11 shows the series of increasing temperatures ("Temperature Difference") between the measuring points in the absorption tube: $T_2 - T_1$, $T_3 - T_2$, $T_4 - T_3$, and $T_4 - T_1$. It can be seen that the total number of temperature differences, " $T_2 - T_1$ " + " $T_3 - T_2$ " + " $T_4 - T_3$ ", was equal to the temperature difference between the temperature sensors, i.e., $T_4 - T_1$. There was a significant temperature difference between T_2 and T_1 compared to points T_2 and T_3 as well as T_3 and T_4 . This was due to the fluid passing through the insulation before entering the absorber tube, which caused a significant difference in

the early stages. However, when the fluid passed through the absorber tube, the flow conditions became more similar, resulting in a lower temperature change in the subsequent period. The experimental results are plotted at different flow rates for the smooth and finned copper tubes. As expected, the temperature difference decreased with an increase in the flow rate, achieving the maximum temperature difference at a flow rate of 0.5 L per minute. It was also found that the temperature difference of the finned tubes was higher than that of the smooth copper tubes, which was true for all the flow rates. This was due to the greater heat-absorbing area of the finned tube. This is consistent with another published study [29,30,70]. Furthermore, the length of the SPT collector affects the temperature difference and efficiency. A longer system will enhance overall efficiency, albeit at the expense of requiring more pumping power due to increased frictional losses.

Table 6. Outlet water temperature of smooth and finned absorber tubes.

Flow Rate (Liters per Minute)	Maximum Water Temperature Smooth Tube (°C)	Maximum Water Temperature Finned Tube (°C)	Difference (°C)	Difference (%)
0.5	56.52	59.34	2.82	4.75
1.0	54.77	56.33	1.56	2.77
2.0	53.87	54.90	1.03	1.88
3.0	52.12	53.80	1.68	3.12
4.0	51.27	51.91	0.64	1.23

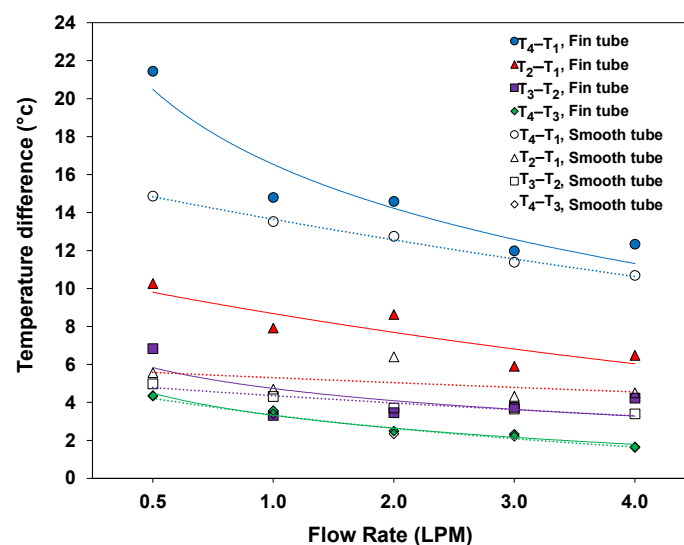


Figure 11. Temperature differences in the collector tubes at different flow rates.

3.3. Useful Energy

Figure 12 shows the heat transfer as a function of the water flow rates for the smooth and finned copper tubes. It can be seen that the heat transfer rate in the smooth absorber tubes was almost constant for all the flow rates; however, there was a significant difference in the finned absorber tubes, especially at lower flow rates. The results show that the finned tubes achieved a heat transfer rate of 1375.55 W at the low flow rate of 0.5 L per minute, 43.9% higher than that of the smooth tubes at the same flow rate. This was because the surface area for absorbing the solar radiation was much larger (due to the fins) than the surface area for the heat transfer between the working fluid and the tube. The results therefore suggest that externally finned tube absorbers need to be operated at low flow rates to maximize their useful energy output. Furthermore, this result illustrates the need for the modelling of the heat transfer in this sort of system, given the fact that conventional correlations are unlikely to be applicable.

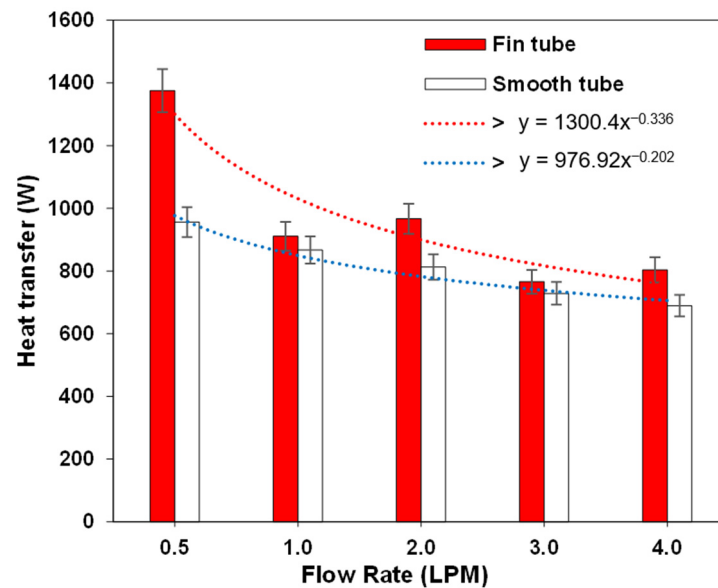


Figure 12. Heat transfer as a function of flow rate for absorber tubes with and without fins.

3.4. Efficiency

Figure 13 shows the thermal efficiency of the SPT collector as a function of the water flow rate for the smooth and finned absorber tubes. The overall efficiency is computed based on the thermal energy generated from a solar receiver compared with solar irradiation. It can be seen that a flow rate of 0.5 L per minute gave a maximum efficiency of 18.2% and 12.3% for the finned and smooth tubes, respectively. This trend was likely due to increased heat losses at higher flow rates. Furthermore, it can be observed that the efficiency was consistently less than 20%, which is well below the expected efficiency of more than 40% [30,71]. However, there were many factors that could contribute to the low efficiency. For example, this low-cost collector was developed using local skills and materials. Other contributory factors to the low efficiency include the refraction of sunlight as well as imperfections in the control mechanisms and movement mechanisms of the system, particularly the accuracy of tracking the solar path of the Sun.

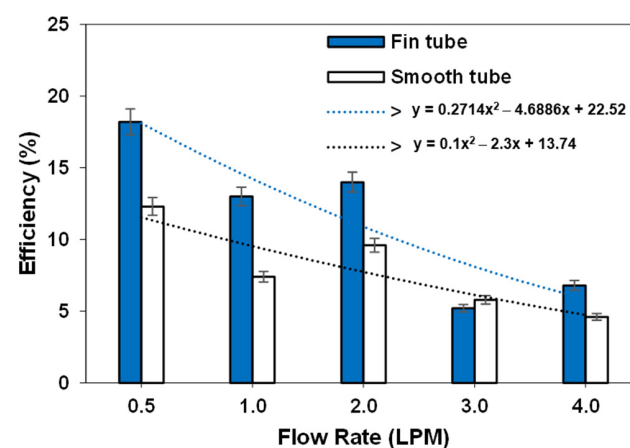


Figure 13. Thermal efficiency of finned and smooth absorber tubes as a function of water flow rate.

ASHRAE standard 93 (2003) [72] was used to estimate the thermal efficiency of the SPT in terms of the input temperature and ambient temperature during steady-state conditions. Equation (25) [73] shows that overall thermal efficiency

$$\eta = F_R \eta_o - \frac{F_R U_L}{CR} \left(\frac{T_{in} - T_a}{G} \right) \quad (25)$$

where F_R is the factor of heat removal, η_o is the optical efficiency, and U_L is the overall loss coefficient.

The results from the experiment were used to plot SPT efficiency curves using standard least squares technical plotting. The slope is the term " $F_R U_L / CR$ ", and the intercept is the term " $F_R \eta_o$ ". From Figure 14, it can be seen that the slope was 0.027 and that the intercept was 0.186. Therefore, the equation for the overall thermal efficiency of the solar parabolic trough collector can be written as

$$\eta = 0.186 - 0.027 \left(\frac{T_{in} - T_a}{G} \right) \quad (26)$$

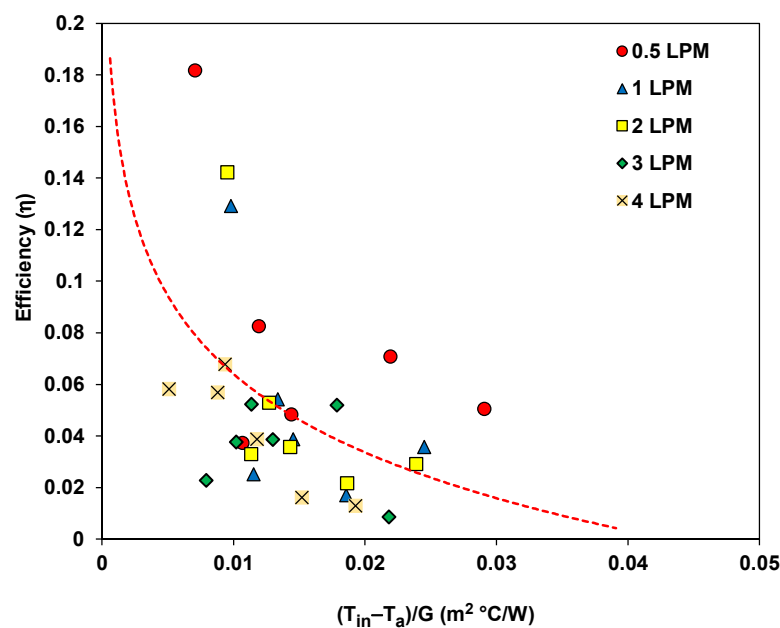


Figure 14. Efficiency of the SPT with finned absorber tube at various flow rates. Least squares fit line shown.

Figure 14 presents a thermal performance curve based on the data collected throughout the experiment. The line of the least squares fit equation is shown in the graph and indicates that the collector had an intercept efficiency of about 18%, which is much lower than expected, as established in earlier studies [74–76] and that it reduced with the flow rate. It can be observed that, as the mass flow rate increased, the term " $(T_{in} - T_a)/G$ " increased, resulting in a decrease in efficiency. Therefore, it can be seen that the change in efficiency depends on the parameter of the temperature difference in the term " $(T_{in} - T_a)/G$ ".

Figure 15 shows that a tube with external fins consistently outperforms a smooth tube in a solar receiver. The trend of the efficiency with the term " $(T_{in} - T_a)/G$ " observed in this study is similar to that found in earlier research [75–77]. It can be observed that the efficiency was much higher at lower values of the term " $(T_{in} - T_a)/G$ ", which further supports the suggestion that a lower performance at higher flow rates is a result of increased heat losses. This is because the losses will be proportional to the temperature difference between the fluid and the ambient air. Additionally, Table 7 compares the efficiency and heat transfer parameters for both cases, finned and smooth tubes. The finned solar absorber tube was about 48% more efficient than the smooth tube, mainly due to improved energy absorption.

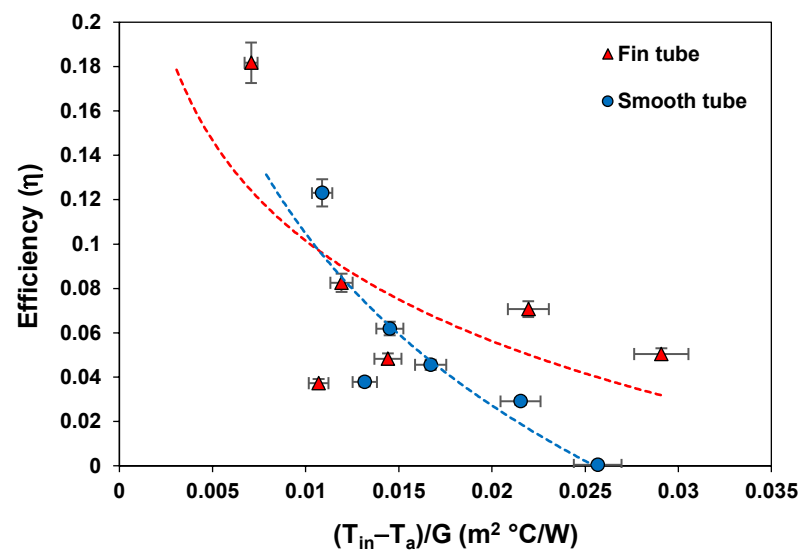


Figure 15. The efficiency of the SPT with reduced temperature for absorber tubes with and without fins at a flow rate of 0.5 L per minute.

Table 7. Comparison of efficiency and heat transfer parameters for both tube types.

Case	Heat Transfer (W)	Maximum Efficiency (%)	Equation
Finned tube	1375.55	18.20	$y = -0.065\ln(x) - 0.1991$
Smooth tube	955.65	12.30	$y = -0.112\ln(x) - 0.4105$

3.5. Environmental Impact Evaluation

In Thailand, fossil fuels account for 91.5% of the nation's total power generation. Natural gas makes up more than 70% of these fossil fuels [78–80]. These fossil fuels are the main source of CO₂ emissions (CO₂e) [79]. The solar parabolic trough system does not directly release carbon dioxide (CO₂) during its operation because it does not use fossil fuels to generate heat. Using Equation (27) [19,81], it is possible to determine how much CO₂ is released during the process of making energy equivalent to that generated by the SPT system:

$$CO_2emissions = Activity\ Data\ (from\ SPT) \times Emission\ Factor \quad (27)$$

where CO₂ emissions (CO₂e) are expressed in kg and where the emission factor is equal to 0.5986 kgCO₂e/kWh [80] for Thailand in this case study.

Figure 16 shows the reduction in the CO₂ emission rate when using the SPT system as a function of the water flow rate for the smooth and finned copper tubes. It can be seen that the reduction in the rate of CO₂ emissions was significantly different in the finned tube, especially at lower flow rates. The results show that the finned tubes offer the possibility to reduce CO₂ emissions by 0.2726 metric tons of CO₂e per year at a low flow rate of 0.5 L per minute; this is about 44% more than that of the smooth tubes (Table 8) at the same flow rate. This is because finned tubes generate more heat energy. Similarly, the results suggest that externally finned tube absorbers need to operate at low flow rates to maximize the useful energy. These results show that the substitution of fossil fuel use with STP systems can help avoid CO₂ emissions (CO₂e) and hence deliver environmental benefits.

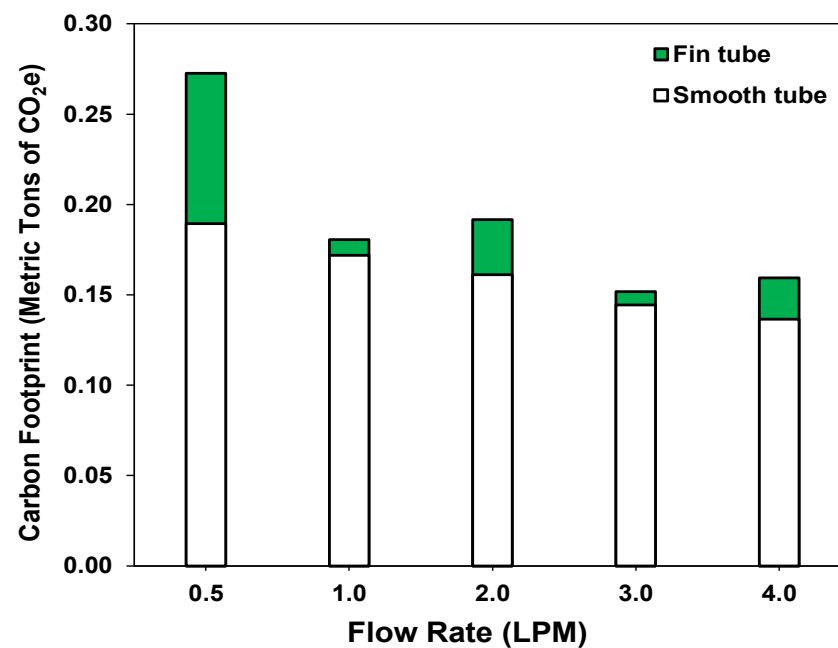


Figure 16. The avoided CO₂ emission rate as a function of flow rate when using an SPT system.

Table 8. The avoided CO₂ emission rate was achieved by using an SPT system for both cases at a flow rate of 0.5 L per minute.

Case	Energy (kWh/day)	Carbon Footprint (Metric Tons of CO ₂ e/day)	Carbon Footprint (Metric Tons of CO ₂ e/Year)	Rate Increase (%)
Finned tube	1.376	0.0007	0.2726	43.92
Smooth tube	0.956	0.0005	0.1894	-

3.6. Cost Analysis of the Solar Parabolic Trough System Projects

The SPT system used in this work was designed and constructed in Thailand. The duration of the project was 20 years. The total initial investment cost was equivalent to USD 10,526.32 at an interest rate of 6.75%. In Table 9, the project's financial analysis results show that the net present value (NPV) was USD 988.87, which is greater than zero. The internal rate of return (IRR) was 9.57%, which is higher than the loan rate. The specified discount rate was 6.75%, and the payback period was approximately 8.77 years, which is within the project's implementation period. Consequently, when comparing the study results with the investment decision criteria, the project was worth the investment.

Table 9. Economic results for the solar parabolic trough system (for this case study).

Energy (kWh/day)	Annual Energy (kWh/year)	Initial Investment (USD)	Year Investor IRR Achieved (Year)	Interest Rate (%) [63]	Weighted Average Cost of Capital, WACC (%) [82]	Net Present Value, NPV (USD)	Internal Rate of Return, IRR (%)	Payback Period, PB (Year)
1.376	502.24	10,526.32	20	6.75	8.31	988.87	9.57	8.77

4. Conclusions

This paper compares the thermal performance of smooth and externally finned absorber tubes used in solar parabolic trough (SPT) receivers. An SPT with a focal length of 300 mm and a length of 5.1 m was designed and built in order to investigate its ability to generate heat using water as a heat transfer fluid at flow rates ranging from 0.5 to 4 L per minute. The water was circulated through solar absorber tubes of two types, specifically, a smooth tube and a tube with external fins. The tubes were placed at the focal point of the parabolic trough. The conclusions of this study include the following:

1. The results show that the externally finned absorber tube demonstrated an improved thermal efficiency of up to 48% over and above that of the smooth absorber tube. This was attributed to the fact that the finned outer surface had more area for energy absorption.
2. The externally finned absorber tube provided a higher fluid exit temperature than the smooth absorber tube at the same flow rate. With a flow rate of 0.5 L per minute, the maximum output temperature from the finned tube was 59.34 °C, which is 2.82 °C more than that of the smooth tube, representing a 4.75% increase.
3. The results also show that, at the low fluid flow rate of 0.5 L per minute, the finned tubes achieved a heat transfer rate of 1375.55 W, which is about 44% more than that of the smooth tubes, with an efficiency of 18.2%, which is around 48% more than that of the smooth tubes.
4. The research found that the experimental SPT system using finned tubes potentially avoided CO₂ emissions to the amount of 0.2726 metric tons of CO₂e per year, with the finned tubes outperforming the smooth tubes by about 44% at a flow rate of 0.5 L per minute.
5. The main conclusion of this paper is that externally finned absorber tubes are an inexpensive and easy-to-manufacture method to significantly improve the thermal performance of SPT systems.

For future works, it is recommended to study parameters for optimizing the geometry of the fins, such as the shapes, widths, thicknesses, and spaces between each fin, including the reflector sheets at both ends of the solar collector. Numerical analyses could be carried out to optimize the geometrical characteristics, which would reduce the time and experimental validation costs.

Author Contributions: Conceptualization, T.L. and M.O.; methodology, T.L. and M.O.; investigation, T.L., M.O. and D.H.; resources, T.L., N.P. and P.B.; data curation, T.L.; writing—original draft preparation, T.L., M.O. and D.H.; writing—review and editing, T.L., M.O., D.H., N.P. and P.B.; supervision, M.O. and D.H. All authors have read and agreed to the published version of the manuscript.

Funding: This research received no external funding.

Data Availability Statement: Not applicable.

Acknowledgments: The authors would like to acknowledge Tirarut Eaumkeb; Satawat Udnoonchart; and the technical staff from the Department of Mechanical Engineering, the Faculty of Engineering, Srinakharinwirot University, Nakhon Nayok, Thailand, for their assistance in this work.

Conflicts of Interest: The authors declare no conflict of interest.

Nomenclature

A_a	(m ²)	Aperture area
A_r	(m ²)	Receiver surface area
A_c	(m ²)	Cross-sectional area of copper tube
C_p	(J/kg·K)	Specific heat capacity
CR	(-)	The geometric concentration ratio
D	(m)	Characteristic diameter dimension
D_{go}	(m)	Outside diameter of glass envelope
D_{gi}	(m)	Inner glass cover diameter
D_{ci}	(m)	Inside diameter of copper tube
D_{co}	(m)	Outside diameter of copper tube
E	(hrs)	Equation of time
F_R	(-)	The factor of heat removal
f	(-)	Focus of parabolic
G	(W/m ²)	Solar radiation
h	(W/m ² K)	The heat transfer coefficient
k	(W/(m·K))	Thermal conductivity

Re	(-)	Reynolds number
st	(-)	Local standard time
I_b	(W/m ²)	The direct solar light intensity
I_{eff}	(W/m ²)	The effective intensity of sunlight
L	(m)	Characteristic linear dimension
L_r	(m)	Receiver length
$Long$	(-)	Longitude
l	(-)	The latitudes on the Earth
\dot{m}	(kg/s)	Mass flow rate of fluid flow
m	(kg)	Mass of fluid
n	(day)	The year's day
N	(-)	North
S	(-)	South
Q	(W)	Thermal power of fluid
Q_{water}	(W)	Daily energy gained from water
Q_s	(W)	Solar energy on the trough aperture
q	(W/m ²)	Heat flux density
T	(°C)	Temperature
t	(s)	Time
U_L	(W/m ² K)	Overall heat loss coefficient
v	(m/s)	Flow speed of fluid
\dot{V}	(m ³ /s)	Volumetric flow rate
P	(-)	The position of a point on the Earth's surface
x	(m)	The distance of the parabolic curve along the X axis
Y_z	(-)	Accuracy of the devices
y	(m)	Curve length of the parabolic
W	(m)	The width of the parabolic collector
Special characters		
w	(°)	The angle of each hour
d	(°)	The Sun's declination angle
θ	(°)	The Sun's incident angle
h	(-)	Overall efficiency
h_o	(-)	Optical efficiency
r	(kg/m ³)	Density of the fluid
α		Reflectance of reflector surface
m	(kg/(m·s))	Dynamic viscosity of the fluid
Subscripts		
st		Longitude drags through the standard time
s		Solar
r		Receiver tube
fm		Mean fluid temperature
$final$		Final water temperature of system
$initial$		Initial water temperature of system
Loc		Longitude drags through the local time
u		Useful
$1-4$		Position temperature
in		Inlet fluid temperature
out		Outlet fluid temperature
a		Ambient temperature
g		Glass receiver tube
t		Water tank temperature
Abbreviations		
AT		Absorber Tube
ASHRAE		American Society of Heating, Refrigerating and Air-Conditioning Engineers
CLFR		Compact linear Fresnel reflector
HTF		The heat transfer fluid
IRR		The internal rate of return
LPM		Liters per minute

NPV	The net present value
PB	Payback period
PDC	Parabolic dish collector
SPT	Solar parabolic trough
SPTC	Solar parabolic trough collector
SWU	Srinakharinwirot University
USD	The currency abbreviation for the U.S. dollar
UTC	Coordinated universal time

Appendix A

Figure A1 shows all the data on solar radiation collected on clear and cloudy days throughout the experiment. It can be seen that experimental data collection was conducted for 20 days. However, 10 days of the data with the least cloud cover were used for the analysis as shown in Figure 8.

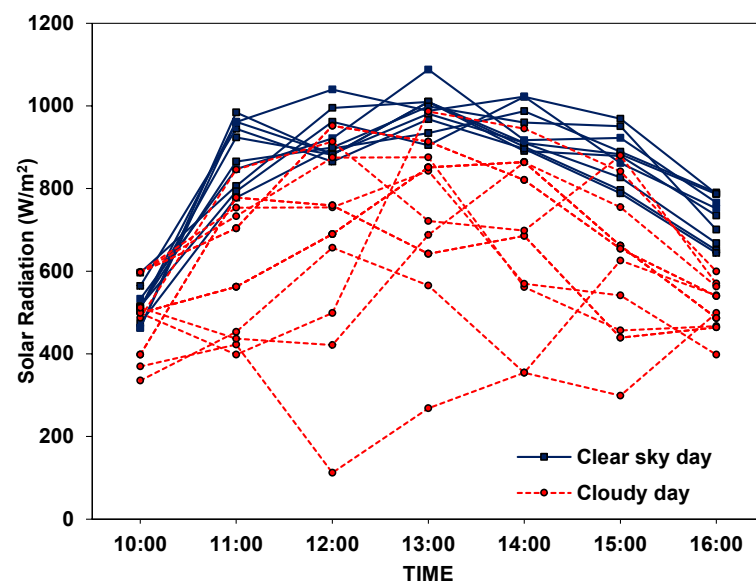


Figure A1. The collection of data on the variation in solar radiation with time on clear and cloudy days.

References

- Balakrishnan, P.S.; Shabbir, M.F.; Siddiqi, A.; Wang, X. Current status and future prospects of renewable energy: A case study. *Energy Sources Part A Recovery Util. Environ. Eff.* **2020**, *42*, 2698–2703. [\[CrossRef\]](#)
- Bamisile, O.; Dagbasi, M.; Babatunde, A.; Ayodele, O. A review of renewable energy potential in Nigeria; solar power development over the years. *Eng. Appl. Sci. Res.* **2017**, *44*, 242–248.
- Garg, H. *Solar Energy: Fundamentals and Applications*; Tata McGraw-Hill Education: New York, NY, USA, 2000.
- Kabir, E.; Kumar, P.; Kumar, S.; Adelodun, A.A.; Kim, K.-H. Solar energy: Potential and future prospects. *Renew. Sustain. Energy Rev.* **2018**, *82*, 894–900. [\[CrossRef\]](#)
- Khan, B. *Non-Conventional Energy Resources*; Tata McGraw-Hill Education: New York, NY, USA, 2006.
- Rai, G. *Non Conventional Energy Sources*; Khanna Publishers: New Delhi, India, 1986.
- Krungkaew, S.; Kingphadung, K.; Kwonpongsagoon, S.; Mahayothee, B. Costs and benefits of using parabolic greenhouse solar dryers for dried herb products in Thailand. *Geomate J.* **2020**, *18*, 96–101. [\[CrossRef\]](#)
- Duffie, J.A.; Beckman, W.A.; Blair, N. *Solar Engineering of Thermal Processes, Photovoltaics and Wind*; John Wiley & Sons: Hoboken, NJ, USA, 2020.
- Badran, O. Study in industrial applications of solar energy and the range of its utilization in Jordan. *Renew. Energy* **2001**, *24*, 485–490. [\[CrossRef\]](#)
- Schiel, W.; Keck, T. Parabolic dish concentrating solar power systems. In *Concentrating Solar Power Technology*; Elsevier: Amsterdam, The Netherlands, 2021; pp. 311–355.
- Price, H.; Forristall, R.; Wendelin, T.; Lewandowski, A.; Moss, T.; Gummo, C. Field survey of parabolic trough receiver thermal performance. In *Proceedings of the International Solar Energy Conference, Dresden, Germany, 4–8 September 2006*; pp. 109–116.

12. Romero, M.; Steinfeld, A. Concentrating solar thermal power and thermochemical fuels. *Energy Environ. Sci.* **2012**, *5*, 9234–9245. [CrossRef]
13. Gong, J.-H.; Wang, J.; Lund, P.D.; Zhao, D.-D.; Hu, E.-Y.; Jin, W. Improving the performance of large-aperture parabolic trough solar concentrator using semi-circular absorber tube with external fin and flat-plate radiation shield. *Renew. Energy* **2020**, *159*, 1215–1223. [CrossRef]
14. Gong, J.-H.; Wang, J.; Lund, P.D.; Zhao, D.-D.; Xu, J.-W.; Jin, Y.-H. Comparative study of heat transfer enhancement using different fins in semi-circular absorber tube for large-aperture trough solar concentrator. *Renew. Energy* **2021**, *169*, 1229–1241. [CrossRef]
15. Shayan, M.E.; Najafi, G.; Ghasemzadeh, F. Advanced study of the parabolic trough collector using aluminum (III) oxide. *Int. J. Smart Grid* **2020**, *4*, 111–116.
16. Bi, Y.; Qin, L.; Guo, J.; Li, H.; Zang, G. Performance analysis of solar air conditioning system based on the independent-developed solar parabolic trough collector. *Energy* **2020**, *196*, 117075. [CrossRef]
17. Kumar, D.; Kumar, S. Analytical performance investigation of parabolic trough solar collector with computed optimum air gap. *Int. J. Energy Environ.* **2015**, *6*, 87.
18. Aseri, T.K.; Sharma, C.; Kandpal, T.C. Estimation of capital costs and techno-economic appraisal of parabolic trough solar collector and solar power tower based CSP plants in India for different condenser cooling options. *Renew. Energy* **2021**, *178*, 344–362. [CrossRef]
19. Praveenkumar, S.; Agyekum, E.B.; Kumar, A.; Ampah, J.D.; Afrane, S.; Amjad, F.; Velkin, V.I. Techno-economics and the identification of environmental barriers to the development of concentrated solar thermal power plants in India. *Appl. Sci.* **2022**, *12*, 10400. [CrossRef]
20. Purohit, I.; Purohit, P. Techno-economic evaluation of concentrating solar power generation in India. *Energy Policy* **2010**, *38*, 3015–3029. [CrossRef]
21. Tahir, S.; Ahmad, M.; Abd-ur-Rehman, H.M.; Shakir, S. Techno-economic assessment of concentrated solar thermal power generation and potential barriers in its deployment in Pakistan. *J. Clean. Prod.* **2021**, *293*, 126125. [CrossRef]
22. Boretti, A. Cost and production of solar thermal and solar photovoltaics power plants in the United States. *Renew. Energy Focus* **2018**, *26*, 93–99. [CrossRef]
23. Pressebox. The First Parabolic trough Plant Using Direct Steam Generation—Delivers Its Full 5 MW of Output to Thailand's Power Network. Available online: <https://www.pressebox.com/pressrelease/solarlite-gmbh-duckwitz/TSE-1-The-first-parabolic-trough-plant-using-direct-steam-generation-delivers-its-full-5-MW-of-output-to-Thailands-power-network/boxid/478604> (accessed on 3 April 2023).
24. Fuqiang, W.; Qingzhi, L.; Huaizhi, H.; Jianyu, T. Parabolic trough receiver with corrugated tube for improving heat transfer and thermal deformation characteristics. *Appl. Energy* **2016**, *164*, 411–424. [CrossRef]
25. Huang, Z.; Li, Z.-Y.; Yu, G.-L.; Tao, W.-Q. Numerical investigations on fully-developed mixed turbulent convection in dimpled parabolic trough receiver tubes. *Appl. Therm. Eng.* **2017**, *114*, 1287–1299. [CrossRef]
26. Huang, Z.; Yu, G.; Li, Z.; Tao, W. Numerical study on heat transfer enhancement in a receiver tube of parabolic trough solar collector with dimples, protrusions and helical fins. *Energy Procedia* **2015**, *69*, 1306–1316. [CrossRef]
27. Peng, H.; Li, M.; Hu, F.; Feng, S. Performance analysis of absorber tube in parabolic trough solar collector inserted with semi-annular and fin shape metal foam hybrid structure. *Case Stud. Therm. Eng.* **2021**, *26*, 101112. [CrossRef]
28. Vengadesan, E.; Thameenansari, S.; Manikandan, E.J.; Senthil, R. Experimental study on heat transfer enhancement of parabolic trough solar collector using a rectangular channel receiver. *J. Taiwan Inst. Chem. Eng.* **2022**, *135*, 104361. [CrossRef]
29. Zhao, Z.; Bai, F.; Zhang, X.; Wang, Z. Experimental study of pin finned receiver tubes for a parabolic trough solar air collector. *Sol. Energy* **2020**, *207*, 91–102. [CrossRef]
30. Bellos, E.; Tzivanidis, C.; Tsimpoukis, D. Multi-criteria evaluation of parabolic trough collector with internally finned absorbers. *Appl. Energy* **2017**, *205*, 540–561. [CrossRef]
31. Jathar, L.D.; Ganesan, S.; Shahapurkar, K.; Soudagar, M.E.M.; Mujtaba, M.; Anqi, A.E.; Farooq, M.; Khidmatgar, A.; Goodarzi, M.; Safaei, M.R. Effect of various factors and diverse approaches to enhance the performance of solar stills: A comprehensive review. *J. Therm. Anal. Calorim.* **2021**, *147*, 4491–4522. [CrossRef]
32. Tayebi, R.; Akbarzadeh, S.; Valipour, M.S. Numerical investigation of efficiency enhancement in a direct absorption parabolic trough collector occupied by a porous medium and saturated by a nanofluid. *Environ. Prog. Sustain. Energy* **2019**, *38*, 727–740. [CrossRef]
33. Atchuta, S.; Sakthivel, S.; Barshilia, H.C. Selective properties of high-temperature stable spinel absorber coatings for concentrated solar thermal application. *Sol. Energy* **2020**, *199*, 453–459. [CrossRef]
34. Joly, M.; Antonetti, Y.; Python, M.; Gonzalez, M.; Gascou, T.; Scartezzini, J.-L.; Schüler, A. Novel black selective coating for tubular solar absorbers based on a sol–gel method. *Sol. Energy* **2013**, *94*, 233–239. [CrossRef]
35. Kasaeian, A.; Daviran, S.; Azarian, R.D. Optical and thermal investigation of selective coatings for solar absorber tube. *Int. J. Renew. Energy Res.* **2016**, *6*, 15–20.
36. Fedkin, M. Parabolic Dish CSP Technology. Available online: <https://www.e-education.psu.edu/eme812/node/648> (accessed on 26 April 2022).
37. Natarajan, S.K.; Thampi, V.; Shaw, R.; Kumar, V.S.; Nandu, R.; Jayan, V.; Rajagopalan, N.; Kandasamy, R.K. Experimental analysis of a two-axis tracking system for solar parabolic dish collector. *Int. J. Energy Res.* **2019**, *43*, 1012–1018. [CrossRef]

38. Wang, K.; He, Y.-L.; Li, P.; Li, M.-J.; Tao, W.-Q. Multi-objective optimization of the solar absorptivity distribution inside a cavity solar receiver for solar power towers. *Sol. Energy* **2017**, *158*, 247–258. [\[CrossRef\]](#)
39. Naphon, P. Experimental investigation the nanofluids heat transfer characteristics in horizontal spirally coiled tubes. *Int. J. Heat Mass Transf.* **2016**, *93*, 293–300. [\[CrossRef\]](#)
40. Navakrishnan, S.; Vengadesan, E.; Senthil, R.; Dhanalakshmi, S. An experimental study on simultaneous electricity and heat production from solar PV with thermal energy storage. *Energy Convers. Manag.* **2021**, *245*, 114614. [\[CrossRef\]](#)
41. Ghasemi, S.E.; Ranjbar, A.A. Numerical thermal study on effect of porous rings on performance of solar parabolic trough collector. *Appl. Therm. Eng.* **2017**, *118*, 807–816. [\[CrossRef\]](#)
42. Reddy, K.; Kumar, K.R.; Ajay, C. Experimental investigation of porous disc enhanced receiver for solar parabolic trough collector. *Renew. Energy* **2015**, *77*, 308–319. [\[CrossRef\]](#)
43. Zheng, Z.; Xu, Y.; He, Y. Thermal analysis of a solar parabolic trough receiver tube with porous insert optimized by coupling genetic algorithm and CFD. *Sci. China Technol. Sci.* **2016**, *59*, 1475–1485. [\[CrossRef\]](#)
44. Mwesigye, A.; Bello-Ochende, T.; Meyer, J.P. Heat transfer and entropy generation in a parabolic trough receiver with wall-detached twisted tape inserts. *Int. J. Therm. Sci.* **2016**, *99*, 238–257. [\[CrossRef\]](#)
45. Song, X.; Dong, G.; Gao, F.; Diao, X.; Zheng, L.; Zhou, F. A numerical study of parabolic trough receiver with nonuniform heat flux and helical screw-tape inserts. *Energy* **2014**, *77*, 771–782. [\[CrossRef\]](#)
46. Zhu, X.; Zhu, L.; Zhao, J. Wavy-tape insert designed for managing highly concentrated solar energy on absorber tube of parabolic trough receiver. *Energy* **2017**, *141*, 1146–1155. [\[CrossRef\]](#)
47. Chakraborty, O.; Roy, S.; Das, B.; Gupta, R. Effects of helical absorber tube on the energy and exergy analysis of parabolic solar trough collector—A computational analysis. *Sustain. Energy Technol. Assess.* **2021**, *44*, 101083. [\[CrossRef\]](#)
48. Muñoz, J.; Abánades, A. Analysis of internal helically finned tubes for parabolic trough design by CFD tools. *Appl. Energy* **2011**, *88*, 4139–4149. [\[CrossRef\]](#)
49. Valizade, M.; Heyhat, M.; Maerefat, M. Experimental study of the thermal behavior of direct absorption parabolic trough collector by applying copper metal foam as volumetric solar absorption. *Renew. Energy* **2020**, *145*, 261–269. [\[CrossRef\]](#)
50. Guerraiche, D.; Bougriou, C.; Guerraiche, K.; Valenzuela, L.; Driss, Z. Experimental and numerical study of a solar collector using phase change material as heat storage. *J. Energy Storage* **2020**, *27*, 101133. [\[CrossRef\]](#)
51. Kaloudis, E.; Papanicolaou, E.; Belessiotis, V. Numerical simulations of a parabolic trough solar collector with nanofluid using a two-phase model. *Renew. Energy* **2016**, *97*, 218–229. [\[CrossRef\]](#)
52. Tripathy, A.K.; Ray, S.; Sahoo, S.S.; Chakrabarty, S. Structural analysis of absorber tube used in parabolic trough solar collector and effect of materials on its bending: A computational study. *Sol. Energy* **2018**, *163*, 471–485. [\[CrossRef\]](#)
53. Abed, N.; Afgan, I.; Cioncolini, A.; Iacovides, H.; Nasser, A.; Mekhail, T. Thermal performance evaluation of various nanofluids with non-uniform heating for parabolic trough collectors. *Case Stud. Therm. Eng.* **2020**, *22*, 100769. [\[CrossRef\]](#)
54. Subramani, J.; Sevvell, P.; Srinivasan, S. Influence of CNT coating on the efficiency of solar parabolic trough collector using Al_2O_3 nanofluids—a multiple regression approach. *Mater. Today Proc.* **2021**, *45*, 1857–1861. [\[CrossRef\]](#)
55. Limboonruang, T.; Phunapai, N.; Oyinlola, M. Experimental investigation of a locally fabricated low-cost solar parabolic trough in Thailand. In Proceedings of the 16th International Conference on Heat Transfer (HEFAT-ATE 2022), Amsterdam, The Netherlands, 8–10 August 2022; pp. 432–437.
56. Kalogirou, S.A. *Solar Energy Engineering: Processes and Systems*; Academic Press: Cambridge, MA, USA, 2013.
57. Lüpfert, E.; Herrmann, U.; Price, H.; Zarza, E.; Kistner, R. Toward standard performance analysis for parabolic trough collector fields. In Proceedings of the SolarPACES Conference, Online, 7 September–1 October 2021.
58. Zou, B.; Dong, J.; Yao, Y.; Jiang, Y. An experimental investigation on a small-sized parabolic trough solar collector for water heating in cold areas. *Appl. Energy* **2016**, *163*, 396–407. [\[CrossRef\]](#)
59. Tzivanidis, C.; Bellos, E.; Korres, D.; Antonopoulos, K.; Mitsopoulos, G. Thermal and optical efficiency investigation of a parabolic trough collector. *Case Stud. Therm. Eng.* **2015**, *6*, 226–237. [\[CrossRef\]](#)
60. Sookramoon, K. Design, construct and performance evaluation of a 2-stage parabolic through solar concentrator in PathumThani. *Adv. Mater. Res.* **2014**, *931–932*, 1291–1297. [\[CrossRef\]](#)
61. Ayodele, T.; Mosetlhe, T.; Yusuff, A.; Ntombela, M. Optimal design of wind-powered hydrogen refuelling station for some selected cities of South Africa. *Int. J. Hydrogen Energy* **2021**, *46*, 24919–24930. [\[CrossRef\]](#)
62. Brigham, E.F.; Houston, J.F. *Fundamentals of Financial Management: Concise*; Cengage Learning: Boston, MA, USA, 2021.
63. Intaraburt, W.; Sangsanont, J.; Limpiyakorn, T.; Ruangrassamee, P.; Suttinon, P.; Suwannasilp, B.B. Feasibility Study of Water Reclamation Projects in Industrial Parks Incorporating Environmental Benefits: A Case Study in Chonburi, Thailand. *Water* **2022**, *14*, 1172. [\[CrossRef\]](#)
64. Praveenkumar, S.; Gulakhmadov, A.; Agyekum, E.B.; Alwan, N.T.; Velkin, V.I.; Sharipov, P.; Safaraliev, M.; Chen, X. experimental study on performance enhancement of a photovoltaic module incorporated with CPU heat pipe—A 5E analysis. *Sensors* **2022**, *22*, 6367. [\[CrossRef\]](#) [\[PubMed\]](#)
65. Janjai, S. A method for estimating direct normal solar irradiation from satellite data for a tropical environment. *Sol. Energy* **2010**, *84*, 1685–1695. [\[CrossRef\]](#)
66. Janjai, S.; Laksanaboonsong, J.; Seesaard, T. Potential application of concentrating solar power systems for the generation of electricity in Thailand. *Appl. Energy* **2011**, *88*, 4960–4967. [\[CrossRef\]](#)

67. Oyinlola, M.; Shire, G. Characterising micro-channel absorber plates for building integrated solar thermal collectors. *Build. Serv. Eng. Res. Technol.* **2019**, *40*, 13–29. [\[CrossRef\]](#)
68. Oyinlola, M.A.; Shire, G.S.; Moss, R. Thermal analysis of a solar collector absorber plate with microchannels. *Exp. Therm. Fluid Sci.* **2015**, *67*, 102–109. [\[CrossRef\]](#)
69. Ali, Z.; Zeeshan, A.; Bhatti, M.; Hobiny, A.; Saeed, T. Insight into the dynamics of Oldroyd-B fluid over an upper horizontal surface of a paraboloid of revolution subject to chemical reaction dependent on the first-order activation energy. *Arab. J. Sci. Eng.* **2021**, *46*, 6039–6048. [\[CrossRef\]](#)
70. Amina, B.; Miloud, A.; Samir, L.; Abdelylah, B.; Solano, J. Heat transfer enhancement in a parabolic trough solar receiver using longitudinal fins and nanofluids. *J. Therm. Sci.* **2016**, *25*, 410–417. [\[CrossRef\]](#)
71. Norouzi, A.M.; Siavashi, M.; Ahmadi, R.; Tahmasbi, M. Experimental study of a parabolic trough solar collector with rotating absorber tube. *Renew. Energy* **2021**, *168*, 734–749. [\[CrossRef\]](#)
72. ANSI/ASHRAE Standard 93-2003; Method of Testing to Determine the Thermal Performance of Solar Collectors. American Society of Heating, Refrigeration and Air Conditioning Engineers: Atlanta, GA, USA, 2003.
73. Arasu, A.V.; Sornakumar, T. Design, manufacture and testing of fiberglass reinforced parabola trough for parabolic trough solar collectors. *Sol. Energy* **2007**, *81*, 1273–1279. [\[CrossRef\]](#)
74. Yousefi, T.; Veisy, F.; Shojaeizadeh, E.; Zinadini, S. An experimental investigation on the effect of MWCNT-H₂O nanofluid on the efficiency of flat-plate solar collectors. *Exp. Therm. Fluid Sci.* **2012**, *39*, 207–212. [\[CrossRef\]](#)
75. Yousefi, T.; Veysi, F.; Shojaeizadeh, E.; Zinadini, S. An experimental investigation on the effect of Al₂O₃-H₂O nanofluid on the efficiency of flat-plate solar collectors. *Renew. Energy* **2012**, *39*, 293–298. [\[CrossRef\]](#)
76. Zamzamian, A.; KeyanpourRad, M.; KianiNeyestani, M.; Jamal-Abad, M.T. An experimental study on the effect of Cu-synthesized/EG nanofluid on the efficiency of flat-plate solar collectors. *Renew. Energy* **2014**, *71*, 658–664. [\[CrossRef\]](#)
77. Jamal-Abad, M.T.; Saedodin, S.; Aminy, M. Experimental investigation on a solar parabolic trough collector for absorber tube filled with porous media. *Renew. Energy* **2017**, *107*, 156–163. [\[CrossRef\]](#)
78. Agency, I.E. *Thailand Electricity Security Assessment*; International Energy Agency: Paris, France, 2016.
79. Choomkong, A.; Sirikunpitak, S.; Darnsawasdi, R.; Yordkayhun, S. A study of CO₂ emission sources and sinks in Thailand. *Energy Procedia* **2017**, *138*, 452–457. [\[CrossRef\]](#)
80. Thailand Greenhouse Gas Management Organization. Carbon Footprint for Organization: CFO, Corporate Carbon Footprint: CCF. Available online: <http://thaicarbonlabel.tgo.or.th> (accessed on 4 April 2023).
81. Aroonsrimorakot, S.; Yuwaree, C.; Arunlertaree, C.; Hutajareorn, R.; Buadit, T. Carbon footprint of faculty of environment and resource studies, Mahidol University, Salaya Campus, Thailand. *APCBEE Procedia* **2013**, *5*, 175–180. [\[CrossRef\]](#)
82. Arjharn, W.; Diloksumpun, S.; Ladpala, P.; Mahuchariyawong, J. Study of the Economy Cost of a Small Scale Biomass Power Plant for Rural Communities. Available online: https://kukr.lib.ku.ac.th/kukr_es/kukr (accessed on 4 April 2023).

Disclaimer/Publisher’s Note: The statements, opinions and data contained in all publications are solely those of the individual author(s) and contributor(s) and not of MDPI and/or the editor(s). MDPI and/or the editor(s) disclaim responsibility for any injury to people or property resulting from any ideas, methods, instructions or products referred to in the content.